ISSN:2790-1688 DOI: 10.56028/aetr.3.1.871

A Constitutive Model For Predicting The Time And Temperature-Moisture-Dependent Behavior Of Nafion Polymers

Wenqing Liu[1],Diankai Qiu[1,2,b]

[1]State Key Laboratory of Mechanical System and Vibration, Shanghai Jiao Tong University, Shanghai, China

[2]Shanghai Key Laboratory of Digital Manufacture for Thin-walled Structures, Shanghai Jiao Tong University, Shanghai, China

[B]email:dkqiu@sjtu.edu.cn

*Corresponding author e-mail: liuwenqingliu@sjtu.edu.cn

Abstract. Proton exchange membrane fuel cell (PEMFC) is a kind of high-performance fuel cell that converts hydrogen energy to electrical energy. As the core component, the proton exchange membrane (PEM) determines the yield strength and influences the performance of the fuel cell. A newly developed constitutive model is developed for predicting the time and temperature-moisture-dependent mechanical behavior. The model is aiming at predicting the stress response of PEM under different strain rates, temperature, and relative humidity. The mechanical behavior of Nafion polymer is tested between 25° C to 80° C, and relative humidity between 30% ~70% through uniaxial tension. Comparing the experimental data with the model prediction shows that the constitutive theory captured the response, especially under different humidity and temperature.

Keywords: PEM, constitutive model, Nafion.

1. Introduction

Polymer electrolyte membrane (PEM) plays an important role in separating fuels and transporting protons during the running process [1]. These materials usually have the main chain of [(– CF2 – CF2 –)n], as well as some bonded ionizable groups, which leads to some unique mechanical properties compared with typical fluoropolymers. It has been found that the failure of fuel cell starts at the membrane, thus the tress-strain behavior of PEM and its dependence on temperature and water content is very important for PEMFCs.

Mechanical degradation may stem from temperature and humidity cycles as well as gas pressure changes occurring in fuel cell operation. These changes cause stress concentration in the membrane, and result in catastrophic membrane failure (perforations, cracks, tears, and pinholes) and therefore lead to deterioration and failure of cells [2]. Ren found large in-plane compressive stresses caused by hydration swelling of the constrained membrane in the fuel cell [3]. Expansion and swelling caused by the cyclic hydrothermal conditions are also vital factors influencing the mechanical degradation [4, 5]. Both Li et al. [6] and Wu et al. [7] performed accelerated stress tests on membranes by applying temperature and tensile cycles and found a rapid gas crossover rise and a quick performance reduction of fuel cells. Besides, we found the constrained membrane underwent cyclic swelling/shrinkage under hygrothermal conditions, and finally failed after cyclic loading [8]. As mechanical degradation is inevitable during the hygrothermal cycles and easily affects the lifetime, understanding the mechanical degradation mechanisms is of great importance.

Mechanical behavior of Nafion has been studied widely in these years [9-12]. In these studies, researchers found that the strain rate, temperature, and hydration would greatly influence the elastic modulus and yield stress. The early study by Weber and Newman has concluded the influence of water on the mechanical behavior of Nafion [10]. Tang concludes a linear elastic model and uses a piecewise function to describe different stages of Nafion [9]. Silberstein uses a transformed

ISSN:2790-1688 DOI: 10.56028/aetr.3.1.871
neo-Hookean model to describe the response of Nafion [13]. Yoon and Huang revealed the nonlinear viscoelastic – viscoplastic property of ionomer membranes, and proposed a model according the eight-chain model, which is often used for thermoplasticity polymers [12]. However, all the models conducted now have not accurately described the stress-strain behavior while the water content changed.

This study is to explain the combined influence of strain rate, temperature, and humidity on the stress-strain response of the Nafion polymer, especially the accuracy under different humidity. Hence, the experiments would focus on the uniaxial response under various conditions. A nonlinear viscoelastic-plastic model is then conducted and compared with the experimental data.

2. Experiments

Commercial Nafion 211 membrane was used in the experiment. The thickness of the membrane is 54 μ m and was stored in a desiccator. Pres-treatment strictly followed the instructions given by Dupont Inc.

The tensile test was performed on a DMA Q800 analyzer shown in Fig.1. The temperature was controlled by an electric heater, and the humidity was adjusted by mixing dry air and saturated air, membranes were placed in the environment chamber for 30minites until it reached stable states. The membrane was stretched at different strain rates, temperatures, and water contents. The membranes were cut into pieces of dog bone shape. The first group of experiments was conducted under 25° C and 30% RH; The second group of experiments was performed under 25° C and 30% relative humidity with different strain rates; the first group experiments was performed under 0.1 s−1 and 30% relative humidity with different temperature; and the first group experiments was performed under 0.1 s−1 and 50° C relative humidity with different relative humidity.

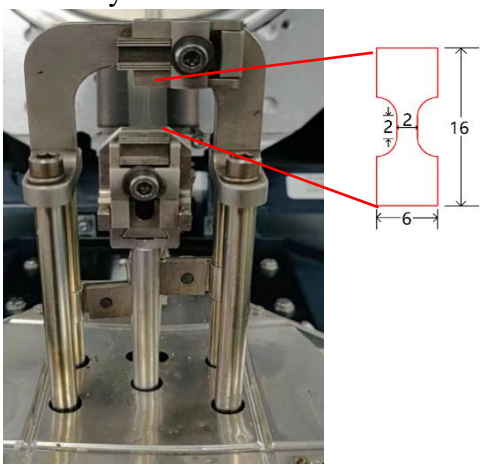

Fig.1 DMA Q800 and the species

3. Constitutive Modeling

PEM exhibits a complicated nonlinear response under loads. At very small deformations, the stress response is nearly linear viscoelastic. At large strains, the material shows a sign of yielding and finally behaves as an unrecoverable deformation.

There are several different models for predicting thermal plastic polymers. As mentioned in the introduction, the modulus of Nafion shows a strong dependence on the water content, so this section will concentrate more on dealing with humidity. The proposed model extends previous work by Bergstrom and Boyce [14, 15] and Silberstein and Boyce [13] for Nafion 211, and tries to improve the accuracy of predicting Nafion’s stress-strain response to different water content.

ISSN:2790-1688 DOI: 10.56028/aetr.3.1.871

In the model, the deformation gradient is divided into two parallel networks: $F = F_A = F_B$ as shown in Fig.2.

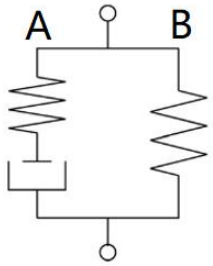

Fig.2 Rheological representation of the model.

The total deformation gradient F_{appl} can be decomposed a hygrothermal expansion part, $F_{th} = \lambda_s I$, where $\lambda_s = 1 + \alpha(\theta - \theta_{ref}) + \beta(\phi - \phi_{ref})$, and a mechanical deformation part F:

$$F^{appl} = FF^{th} \quad (1)$$

In isotropic swelling conditions, $\lambda_s = \left(1 + \varphi \frac{M_{water}}{M_{membrane}}\right)^{\frac{1}{3}} \approx \left(1 + \frac{\varphi}{\rho_1}\right)^{\frac{1}{3}}$,

then the hygro expansion coefficient β, is defined as $\beta = (\partial \ln \lambda_s / \partial \phi)$

The deformation gradient exerting upon Network A can be divided into two parts, F_A^e and F_A^v:

$$F_A = F_A^e F_A^v \quad (2)$$

The Cauchy stress in Network A is given by:

$$\sigma_A = f_a(\theta) \cdot f_c(\phi) \left[\frac{\mu_A}{\lambda_s J_A^e} \mathrm{dev}[b_A^{e*}] + \kappa (J_A^e - 1) I\right] \quad (3)$$

The Cauchy stress on network B is:

$$\sigma_B = f_a(\theta) \cdot f_c(\phi) \left[\frac{\mu_B}{\lambda_s J} \mathrm{dev}[b^*] + \kappa (J - 1) I\right] \quad (4)$$

and the temperature factor $f_a(\theta)$ is given by

$$f_a(\theta) = \begin{cases} f_1, & \theta < \theta_1 \\ f_2, & \theta \geq \theta_2 \\ f_1 + (f_2 - f_1) \cdot (\theta - \theta_1) / (\theta_2 - \theta_1), & \theta_1 \leq \theta < \theta_2 \end{cases} \quad (5)$$

The water correction function $f_c(\phi)$ is given by:

$$f_c(\phi) = (1 - f_5) \exp\left[-\frac{\phi - \phi_{ref}}{f_6}\right] + f_5 \quad (6)$$

The parameter f_5 should be between 0 and 1.

Using this representation the total Cauchy stress is given by

$$\sigma = \sigma_A + \sigma_B \quad (7)$$

The velocity gradient of Network A, $L_A = \dot{F}_A F_A^{-1}$, can be decomposed into elastic and viscous components:

$$\begin{aligned} L_A &= \left[\frac{d}{dt} F_A^e F_A^v\right] (F_A^e F_A^v)^{-1} \quad (8) \\ &= \left[\dot{F}_A^e F_A^v + F_A^e \dot{F}_A^v\right] (F_A^v)^{-1} (F_A^e)^{-1} \\ &= \dot{F}_A^e (F_A^e)^{-1} + F_A^e \dot{F}_A^v (F_A^v)^{-1} (F_A^e)^{-1} \\ &= L_A^e + F_A^e L_A^v (F_A^e)^{-1} \\ &= L_A^e + \tilde{L}_A^v \end{aligned}$$

Where

$$\begin{aligned} L_A^v &= \dot{F}_A^v (F_A^v)^{-1} = D_A^v + W_A^v \\ \tilde{L}_A^v &= \tilde{D}_A^v + \tilde{W}_A^v \end{aligned} \quad (9)$$

To make the unloading unique, prescribe $\tilde{W}_A^v = 0$. The rate of viscous deformation of network A is given by:

$$\tilde{D}_A^v = \dot{\gamma}_A(\sigma_A, b_A^{e*}) N_A^v \quad (10)$$

ISSN:2790-1688 DOI: 10.56028/aetr.3.1.871

where

$$N_A^v = \frac{\mathrm{dev}[\sigma_A]}{\tau} = \frac{\mathrm{dev}[\sigma_A]}{\|\mathrm{dev}[\sigma_A]\|_F} \quad (11)$$

The deformation gradient F_A^v can be derived as follows:

$$\tilde{L}_A^v = \tilde{D}_A^v = \dot{\gamma}_A N_A^v \quad (12)$$

$$\Rightarrow F_A^e \dot{F}_A^v (F_A^v)^{-1} (F_A^e)^{-1} = \dot{\gamma}_A N_A^v$$

$$\Rightarrow \dot{F}_A^v = \dot{\gamma}_A (F_A^e)^{-1} \frac{\mathrm{dev}[\sigma_A]}{\|\mathrm{dev}[\sigma_A]\|_F} F_A^e F_A^v$$

The time derivative for viscous flow is:

$$\dot{\gamma}_A = \dot{\gamma}_0 \exp\left[-\frac{\Delta G}{k_b \theta}\right] \sinh\left[\frac{\Delta G}{k_b \theta} \cdot \frac{\tau}{(r_y + r_i) f_b(\theta) f_d(\phi)}\right] \quad (13)$$

where the temperature factor $f_b(\theta)$ is given by

$$f_b(\theta) = \begin{cases} f_3, & \theta < \theta_3 \\ f_4, & \theta \geq \theta_4 \\ f_3 + (f_4 - f_3) \cdot (\theta - \theta_3) / (\theta_4 - \theta_3), & \theta_3 \leq \theta < \theta_4 \end{cases} \quad (14)$$

The water correction function $f_d(\phi)$ is given by:

$$f_d(\phi) = (1 - f_7) \exp\left[-\frac{\phi - \phi_{ref}}{f_8}\right] + f_7 \quad (15)$$

The parameter f_7 should be between 0 and 1. The effective stress driving the viscous flow is:

$$\tau = \|\mathrm{dev}[\sigma_A]\|_F = \sqrt{\mathrm{tr}[\sigma'_A \sigma'_A]} \quad (16)$$

The yield evolution parameter r_y is given by:

$$\dot{r}_y = h \cdot \left(1 - \frac{r_y}{r_{max}}\right) \dot{\gamma}_A \quad (17)$$

At time t = 0 the yield evolution parameter $r_y = r_0$, as $t \to \infty$, $r_y = r_{max}$, and $\dot{r}_y = 0$.

The intermolecular shear resistance factor is given by:

$$r_i = g \cdot (\lambda_{chain}^n - 1) \quad (18)$$

where g and n are material parameters, and

$$\lambda_{chain} = \sqrt{\frac{\mathrm{tr}[b]}{3}} \quad (19)$$

4. Result and Discussion

Based on the experiment results, we adjusting model parameters according to the testing data, as shown in table 1.

Table 1.Material parameters of the model

Index	Symbol	Unit*	Description	Value
1	A	S	Shear modulus of network A	155.212552
2		S	Bulk modulus	37379.4397
3		T	Reference temperature 1	333.710371
4	f1	-	Temperature factor 1	0.854018737
5		T	Reference temperature 2	388.016921
6	f2	-	Temperature factor 2	0.086280041

ISSN:2790-1688 DOI: 10.56028/aetr.3.1.871

7	$\bar{}$	f	Attempt frequency	0.186347718
8	G/k	T	Activation volume	5.02213954
9	$\hat{\tau}$	S	Flow resistance	6.3012595
10		T	Reference temperature 3	314.355444
11	f3	-	Temperature factor 3	0.230379
12		T	Reference temperature 4	311.458822
13	f4	-	Temperature factor 3	0.0656603224
14	h	-	Evolution rate of flow evolution	412025583.1
15	r0	-	Initial flow evolution value	4.61673851
16	rmax	-	Final flow evolution factor	1.99935265
17	g	-	Global interaction parameter 1	2.68964519
18	n	-	Global interaction parameter 2	1
19		S	Shear modulus of network B	8.91171239
20	ref	T	Reference temperature for thermal expansion	123.159921
21		1/T	Linear thermal expansion coefficient	0.000123
22	ref	-	Reference moisture concentration	
23		-	Coefficient of hygro-expansion	Changed with current
24	f5	-	Water content factor 5 (for moduli)	0.559138418
25	f6	-	Water content factor 6 (for moduli)	5.27331528
26	f7	-	Water content factor 7 (for yield)	0.453891565
27	f8	-	Water content factor 8 (for yield)	5.668889

*where: -=dimensionless, S=stress, T=temperature, f=frequency

The response of the model is compared to experimental data in Fig.3 [11]. The model can capture the stress-strain response under different temperature and hydration. Moreover, the constitutive model could predict the combined influence of changes in both temperature and hydration, especially the accuracy in different humidity.

ISSN:2790-1688 DOI: 10.56028/aetr.3.1.871

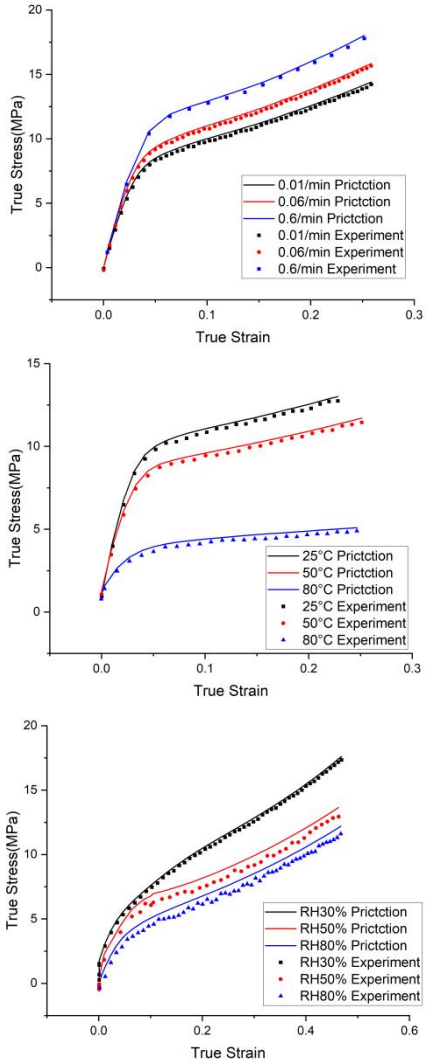

Fig.3 Response in uniaxial extension at different strain rate, temperature, and humidity

5. Conclusion

The stress-strain response of membranes is very complex under varying loads, temperatures, and water content. In this study, we performed a series of experiments on Nafion under different conditions. And developed a model based on existing research. The mechanical behavior was seen to highly depend on strain rate, temperature, and humidity. This model captured the time and temperature-moisture-dependent mechanical behavior and especially improved the accuracy of humidity influence. Further studies will be focused on the parametric analysis, and the mechanical behavior under cyclic loading is also needed.

References

[1] Hong, P., et al., Modeling of membrane electrode assembly of PEM fuel cell to analyze voltage losses inside. Energy, 2017. 139: p. 277-288.

[2] Page, K.A., et al., In Situ Method for Measuring the Mechanical Properties of Nafion Thin Films during Hydration Cycles. ACS Appl Mater Interfaces, 2015. 7(32): p. 17874-83.

[3] Ren, P., et al., Degradation mechanisms of proton exchange membrane fuel cell under typical automotive operating conditions. Progress in Energy and Combustion Science, 2020. 80.

[4] Ye, D., et al., Effects of Frame Materials and Structures on Stress Concentration of Membrane Electrode Assembly of PEMFCs. Fuel Cells, 2013. 13(6): p. 1205-1212.

ISSN:2790-1688 DOI: 10.56028/aetr.3.1.871
[5] Kim, T.-H., et al., Influence of the Nafion agglomerate morphology on the water-uptake behavior and fuel cell performance in the proton exchange membrane fuel cells. Applied Surface Science, 2019. 481: p. 777-784.

[6] Li, B., et al., Mixed Hydrocarbon/Fluoropolymer Membrane/Ionomer MEAs for Durablity Studies. ECS Transactions, 2010. 33(1): p. 913-924.

[7] Wu, B., et al., The degradation study of Nafion/PTFE composite membrane in PEM fuel cell under accelerated stress tests. International Journal of Hydrogen Energy, 2014. 39(26): p. 14381-14390.

[8] Qiu, D., et al., Mechanical failure and mitigation strategies for the membrane in a proton exchange membrane fuel cell. Renewable and Sustainable Energy Reviews, 2019. 113.

[9] Tang, Y., et al., Mechanical properties of a reinforced composite polymer electrolyte membrane and its simulated performance in PEM fuel cells. Journal of Power Sources, 2008. 175(2): p. 817-825.

[10] Weber, A.Z. and J. Newman, Transport in Polymer-Electrolyte Membranes: II. Mathematical Model. Journal of The Electrochemical Society, 2004. 151(2): p. A311-A325.

[11] Silberstein, M.N. and M.C. Boyce, Hygro-thermal mechanical behavior of Nafion during constrained swelling. Journal of Power Sources, 2011. 196(7): p. 3452-3460.

[12] Yoon, W. and X. Huang, A nonlinear viscoelastic–viscoplastic constitutive model for ionomer membranes in polymer electrolyte membrane fuel cells. Journal of Power Sources, 2011. 196(8): p. 3933-3941.

[13] Silberstein, M.N. and M.C. Boyce, Constitutive modeling of the rate, temperature, and hydration dependent deformation response of Nafion to monotonic and cyclic loading. Journal of Power Sources, 2010. 195(17): p. 5692-5706.

[14] Bergström, J.S. and M.C. Boyce, Constitutive modeling of the large strain time-dependent behavior of elastomers. Journal of the Mechanics and Physics of Solids, 1998. 46(5): p. 931-954.

[15] Bergström, J. and L. Hilbert, A constitutive model for predicting the large deformation thermomechanical behavior of fluoropolymers. Mechanics of Materials, 2005. 37(8): p. 899-913.